Supplemental Information for

Tunneling Desorption of Single Hydrogen on the Surface of Titanium Dioxide

Taketoshi Minato[1, 2], Seiji Kajita[3] Chi-Lun Pang[4], Naoki Asao[5],
Yoshinori Yamamoto[5], Takashi Nakayama[3], Maki Kawai[6], Yousoo Kim[2]

[1]*International Advanced Research and Education Organization, Tohoku University, Sendai 980-8578, Japan.*
[2]*Surface and Interface Science Laboratory, RIKEN, 2-1 Hirosawa, Saitama, 351-0198, Japan.*
[3]*Department of Physics, Chiba University, 1-33 Yayoi, Inage, Chiba 263-8522, Japan.*
[4]*Department of Chemistry, University College London,WC1H 0AJ, United Kingdom.*
[5]*WPI Advanced Institute for Materials Research, Tohoku University, 2-1-1 Katahira, Sendai 980-8577, Japan.*
[6]*Department of Advanced Materials Science, The University of Tokyo, 5-1-5 Kashiwanoha, Kashiwa, Chiba 277-8561, Japan.*

§1. Experimental details and theoretical methods

The experiments were performed using a low-temperature STM system (Omicron GmbH) consisting of two chambers separated by a gate valve. TiO_2(110) single crystals (Shinkosha Co. Ltd.) were transferred to the preparation chamber without any pre-treatment. The TiO_2(110) samples were cleaned in the preparation chamber (base pressure: 7×10^{-7} Pa) *via* cycles of Ar^+ sputtering (at 1 keV and 10 μA for 10 min) and annealing (at 900 K for 10 min). After cleaning, the TiO_2(110) was transferred to the STM chamber (base pressure: 4×10^{-9} Pa), where it was placed on a gas-dosing stage. A small amount (1×10^{-8} Pa for 3 sec) of H_2O (or D_2O) was introduced to the dosing stage at room temperature to allow H (or D) to form on the surface. After H_2O (or D_2O) exposure, the TiO_2(110) was transferred to the STM stage, which was maintained at 78 K. All STM results were obtained using electrochemically etched tungsten tips.

To record the action spectroscopy measured *via* STM (STM-AS), the STM tip was placed above the H (or D) on the TiO_2(110) surface while an electrical bias was applied. The tunneling current (I) was monitored using an oscilloscope while the bias was applied. The I signal decreased rapidly when desorption of H (or D) from the TiO_2(110) surface occurred. The reaction yields (Y) and reaction rates (R) were calculated as follows:

$$\mathrm{Y} = \frac{e}{\mathrm{I} \times \mathrm{t}}$$

$$\mathrm{R} = \frac{1}{\mathrm{t}}$$

where *e* is the elementary charge and t is the duration of the applied electric bias, calculated from the onset of the applied bias until desorption. The error bars of Y (Y_{error}), R (R_{error}) and I (I_{error}) in Figure 2 and Figure S2 were calculated as follows:

$$\mathrm{Y_{error}} = \pm\sqrt{\frac{1}{\mathrm{N}}\sum_{\mathrm{i}=1}^{\mathrm{N}}(\mathrm{Y_i} - \mathrm{Y_{av.}})^2}$$

$$\mathrm{R_{error}} = \pm\sqrt{\frac{1}{\mathrm{N}}\sum_{\mathrm{i}=1}^{\mathrm{N}}(\mathrm{R_i} - \mathrm{R_{av.}})^2}$$

$$\mathrm{I_{error}} = \pm\sqrt{\frac{1}{\mathrm{N}}\sum_{\mathrm{i}=1}^{\mathrm{N}}(\mathrm{I_i} - \mathrm{I_{av.}})^2}$$

where N is the total number of data; Y_i, R_i and I_i are the values of Y, R, and I in each measurement; and $Y_{av.}$, $R_{av.}$, and $I_{av.}$ are the average values of Y, R, and I.

DFT calculations were performed using the Tokyo Ab-initio Program Package (TAPP)[1]. We employed the Perdew-Burke-Ernzefhof (PBE) functional as the exchange-correlation term[2], ultrasoft pseudopotentials to describe the ionic cores[3] and a plane-wave basis set with a cut-off energy of 25 Ryd to expand the wave functions of the valence electrons. The TiO_2(110) surface was modeled using a repeated (1×2) slab composed of five TiO_2 trilayers separated by a vacuum space equivalent to 1.3 nm. A single H was adsorbed onto the surface O site of the slab. A ($4 \times 4 \times$

1) Monkhorst-Pack mesh was used for k-point sampling in the Brillouin zone[4]. The slab was relaxed until the force on each atom was below 0.005 Hartree/a.u. with the center trilayer of the slab held frozen in the optimized geometry. The reliability of the parameters was confirmed by evaluating the lattice parameters, and the discrepancy with respect to the experimental values was found to be less than 3%. The field-induced charge-sheets (FICS) method was implemented in the DFT calculations to examine the effect of an applied electric field[5]. In this method, electrons are subtracted from the slab to model positively charged surfaces, and negatively charged counter sheets are inserted into the vacuum regions to maintain overall charge neutrality. Unrealistic interactions between the repeated charged slabs are effectively removed by artificially inserting counter sheets into vacuum regions because the density of the counter sheets varies to screen the electric field of the charged slab. Thus, one can accurately calculate the total energy and electronic states of charged surfaces. The FICS method offers several advantages in terms of the stability of the convergence in the electronic states, its ease of implementation and its accuracy compared with other methods of charged-surface calculation[6-8]. We set a parameter of width of the counter sheets at 0.5 Bohr.

§2. Electronic structure of H/TiO_2(110)

Figure S1 presents scanning tunneling spectra (STS) of H/TiO_2(110) for a range of different sample-tip distances. On TiO_2(110), which is an n-type semiconductor, STS spectra acquired with positive sample bias exhibit an energy shift as a function of the sample-tip distance because of tip-induced band bending[9-12]. No electronic states corresponding to the threshold energies observed in the STM-AS results (Fig. 2) are observable. This finding demonstrates that the STM-tip-induced H desorption from TiO_2(110) is not caused by the excitation of an anti-bonding state.

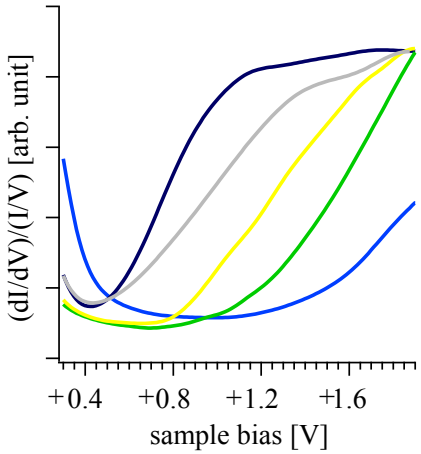

Figure S1. Scanning tunneling spectra obtained on H/TiO_2(110) for various tip-sample distances. Blue curve: tip displacement (TD) = 0 nm (V_s = +1.0 V and I_t = 0.02 nA); green curve: TD = -0.04 nm; yellow curve: TD = -0.10 nm; gray curve: TD = -0.14 nm; purple curve: TD = -0.20 nm. All spectra were normalized by dividing by I/V.

§3. Reaction order of H desorption on TiO_2(110)

The reaction barrier for H desorption on TiO_2(110) is 3.7 eV (Fig. 3). Multiple excitations are necessary to overcome the reaction barrier *via* vibrational excitation because no single vibrational excitation is higher than 3.7 eV (*e.g.,* the OH stretching vibration of H/TiO_2(110) is only 0.457 eV[12]). Figure S2 presents the reaction rates and reaction yields of hydrogen desorption from the TiO_2(110) surface at V_s = +1.6 V. From these results, the reaction order (N) of this reaction was found to be 1.0571. This means that the reaction occurs *via* single-electron excitation and that the desorption of H from TiO_2(110) is not induced by multiple vibrational excitations.

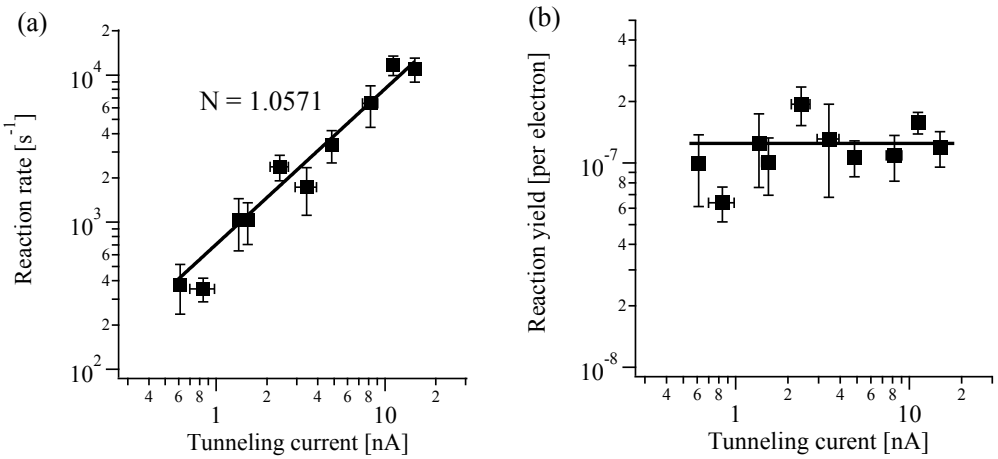

Figure S2. (a) Reaction rates and (b) reaction yields of H desorption from the TiO_2(110) surface obtained at V_s = +1.6 eV.

§4. Reduction of the barrier width for H desorption on TiO_2(110)

When an electric field (positive sample bias) is applied to TiO_2(110), the width of the reaction barrier for H desorption is reduced, as indicated by the arrows in Fig. 3. These features can be explained by the following mechanisms due to the two effects of the electronic field on the potential curve.

In the neutral state of the hydrogenated TiO_2(110) surface, the H on the O_b site forms $(H\text{-}O_b)^-$, which indicates an excess electron associated with the H is provided to the surface. Based on charge-distribution analysis (Fig. S3a), this excess electron redistributes onto Ti sites beneath the O_b sites, and consequently it weakens the ionic bonds between Ti^{4+} and O_b^{2-}. In the process of the H desorption, the O_b is also displaced toward the vacuum to keep the form $(H\text{-}O_b)$ unit.

When a positive electric field is applied on the surface, in the region around the +0.30 nm (or larger than +0.30 nm) displacement of the H in Fig. 3, the protonated H is completely separated from the O_b^{2-}. The desorption H takes an energy gain by the positive electrostatic filed. This energy gain accounts for the reduction of the barrier width in this region. In the region around the +0.15 nm (or shorter than +0.15 nm) displacement of the H, the positively charged surface decreases the amount of the excess electron on the Ti sites, because the excess electron lies nearest to the Fermi level of the H/TiO_2(110) system (as a typical example, in case of no displacement of H is indicated in Fig. S3b). This decrease of the excess electrons causes a recovery in the stiffness of the weakened O_b-Ti ion bond; that is, the Ti sites are able to stretch more to follow the desorbing $(H\text{-}O_b)$ unit. Indeed, Fig. S4 presents that the elongation of bond length between Ti and O_b of O_bH in the H desorption process is suppressed by the positively charged effect. The flexibility of the Ti sites in the desorption process enhances the electrostatic energy gain because the Ti^{4+} sites is close to the counter STM tip that is charged up negatively. Thus, the barrier width is reduced by applying a positive charge on the TiO_2 surface.

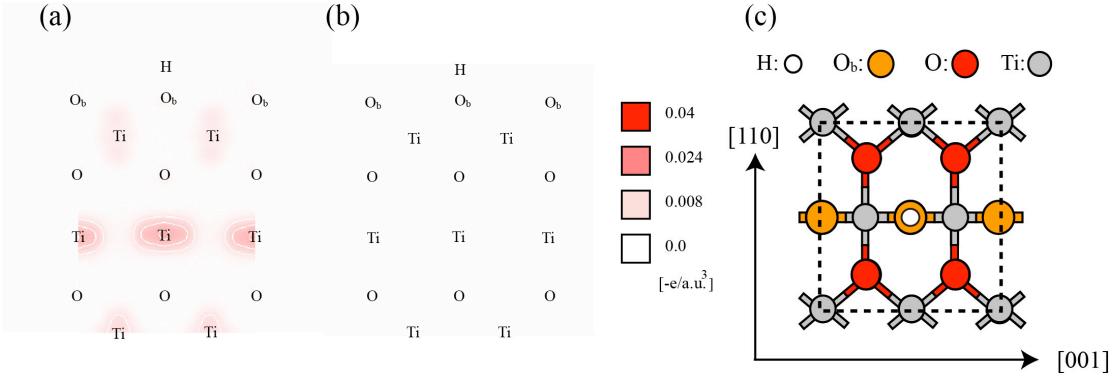

Fig. S3. Distribution of excess electron (a) in the neutral state and (b) in applying 4.5 V/nm electric field on H/TiO_2(110). In (b), the density of the excess electron is decreased. These figures are obtained by subtraction of the electron distribution of the clean TiO_2 surface from that of the H/TiO_2 surface. The cross section in (a) and (b) go along the O_b line in the surface normal direction, that is denoted by the horizontal line in (c).

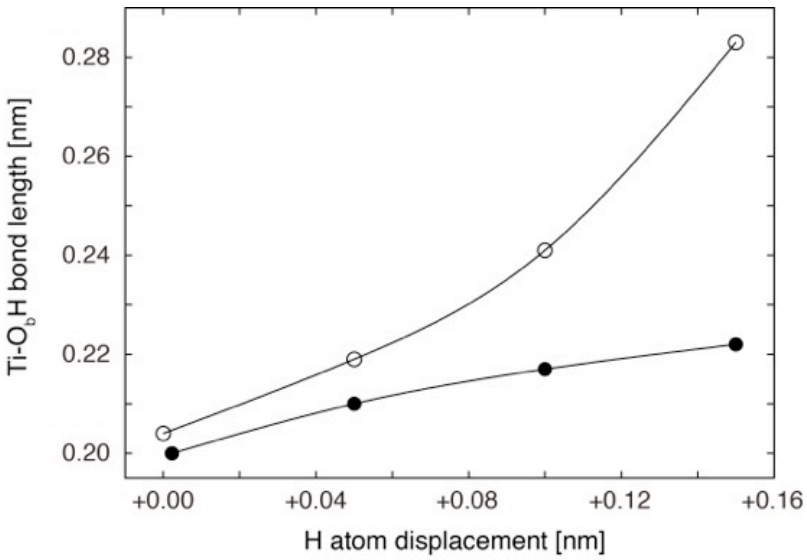

Fig. S4. Variations of the bond length between Ti and O_b of O_bH in the H desorption process. Open circles: 0.0 V/nm; filled circles: 4.5 V/nm.

§5. Effects of the STM tip on the desorption of H from TiO_2(110)

The H that desorbs from the TiO_2(110) adsorbs on the STM tip. Therefore, the effects of the tip on the potential curve for H desorption must be considered. As the tip approaches the TiO_2(110) surface, the potential curves for H on TiO_2 and on the tip begin to cross. The crossing of the potential curves decreases the height of the reaction barrier for H desorption, thus increasing the tunneling probability for H desorption. However, if the effect of the tip on the potential curve only determines the reaction barrier, then the threshold energies observed in the STM-AS measurements (Fig. 2) at a fixed tip-sample distance should be triggered by the excitation of electronic or vibrational states by the tunneling electrons. As shown in Fig. S1, no electronic states were observed in the STS results at the STM-AS threshold energies. As for vibrational excitation, the observed threshold energies (1.2 – 2.0 eV = 9679 – 16131 cm^{-1}) are too large for the vibrational states of H/TiO_2(110). These results indicate that the reaction barrier is not only determined by the effects of STM tip on the potential curve of the H desorption on TiO_2(110).

§6. Tunneling probability of H desorption

The model from which Eq. 1 is derived is explained in detail here. For an isotopic analysis of the tunneling desorption, we used a simple energy-potential well model under an applied electric field, as illustrated in Fig. S5. In this model, the hydrogen on TiO_2(110) is a positive ion. We assume that the protonated hydrogen has a charge of $+\alpha e$ and is bound within a potential well, in which the potential inside the TiO_2(110) is represented by an infinite wall and there is an energy barrier of V_0, representing the desorption energy, at $x = 0$. In the region of $x > 0$, an electric field, E, is applied between the TiO_2(110) and the STM tip. We assume that the hydrogen receives energy, ε, from the tunneling electrons from the STM tip and that the received energy is converted into the excitation of hydrogen vibrations. Here, we use a classical limit of quantum theory called the Wentzel-Kramers-Brillouin (WKB) approximation[13]. The probability of the hydrogen tunneling toward $x > 0$ can be written as follows:

$$\mathrm{T} = \exp\left[-\frac{4\pi}{h}\int_0^a dx\sqrt{2m(-\alpha eEx + \mathrm{V}_0 - \varepsilon)}\right] \quad -(S1)$$

where h is the Planck constant, m is the mass of hydrogen, and a is its position after the tunneling reaction. Equation S1 can be solved analytically as follows:

$$\mathrm{T} = \exp\left\{-\frac{8\pi\sqrt{2m}}{3h\alpha eE}(V_0 - \varepsilon)^{\frac{3}{2}}\right\}.$$

This equation is the same as Eq. 1 in the main text.

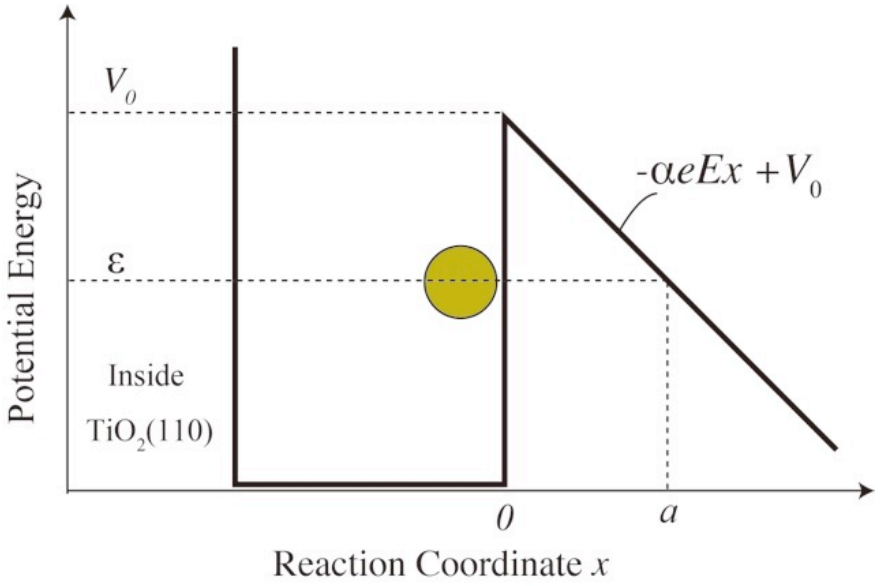

Figure S5. Schematic potential-energy diagram used in the estimation of the tunneling probability for hydrogen desorption. The yellow ball represents the terminal hydrogen on TiO_2(110).

§7. Saturation of the energy shift and the origin of the threshold energies in the STM-AS measurements

The saturation of the shift in the STM-AS threshold energies as the tip approaches the surface (Fig. 2) cannot be completely understood thus far. One possible explanation is that as the STM tip (tungsten (W)) approaches the sample, the tip makes a chemical bond with the H on the TiO_2(110). As the tip continues to draw closer, the W-H-O bond distorts. This distortion may not affect the H desorption behavior. Therefore, the STM-AS measurements do not shift as the tip continues to approach.

Moreover, the origins of the two threshold energies observed in the STM-AS results also remain unclear. The threshold energies observed at a fixed tip-sample distance (Fig. 2) are not directly related to electronic or vibrational states. The reduction of the width of the reaction barrier by electric field would be related to the two threshold energies.

References

[1]Yamauchi, J.; Tsukada, M.; Watanabe, S.; Sugino, O.; First-Principles Study on Energetics of c-BN(001) Reconstructed Surfaces. *Phys. Rev. B* **1996**, *54*, 5586-5602.

[2] Perdew, J. P.; Burke, K.; Ernzerhof, M.; Generalized Gradient Approximation made Simple. *Phys. Rev. Lett.* **1996**, *77*, 3865-3868.

[3] Vanderbilt, D.; Soft Self-Consistent Pseudopotentials in a Generalized Eigenvalue Formalism. *Phys. Rev. B* **1990**, *41*, 7892-7895.

[4] Monkhorst, H. J.; Pack, J. D.; Special Points for Brillouin-Zone Integrations. *Phys. Rev. B* **1976**, *13*, 5188-5192.

[5] Kajita, S.; Nakayama, T.; Kawai, M.; Ab-initio Calculation Method for Electronic Structures of Charged Surfaces using Repeated Slab and Density-Variable Charge Sheets. *J. Phys. Soc. Jpn*. **2007**, *76*, 044701.

[6] Fu, C. L.; Ho, K. M.; External-Charge-Induced Surface Reconstruction on Ag(110). *Phys. Rev. Lett*. **1989**, *63*, 1617-1620.

[7] Kajita, S.; Nakayama, T.; Yamauchi, J.; Density Functional Calculation of Work Function using Charged Slab Systems. *J. Phys.: Conf. Ser*. **2006**, *29*, 120-123.

[8] Otani, M.; Sugino, O.; First-Principles Calculations of Charged Surfaces and Interfaces: A Plane-Wave Nonrepeated Slab Approach. *Phys. Rev. B* **2006**, *73*, 115407.

[9] Batzill, M.; Katsiev, K.; Gaspar, D. J.; Diebold, U.; Variations of the Local Electronic Surface Properties of TiO_2(110) induced by Intrinsic and Extrinsic Defects. *Phys. Rev. B* **2002**, *66*, 235401.

[10] Yoshida, S.; Kanitani, Y.; Oshima, R.; Okada, Y.; Takeuchi, O.; Shigekawa, H.; Microscopic Basis for the Mechanism of Carrier Dynamics in an Operating p-n Junction Examined by Using Light-Modulated Scanning Tunneling Spectroscopy. *Phys. Rev. Lett.* **2007**, *98*, 026802.

[11] Minato, T.;□Sainoo, Y.; Kim, Y.; Kato, H. S.; Aika, K.-i.; Kawai, M.; Zhao, J.; Petek, H.; Huang, T.; He, W.; Wang, B.; Wang, Z.; Zhao, Y.; Yang, J.; and Hou, J. G.; The Electronic Structure of Oxygen Atom Vacancy and Hydroxyl Impurity Defects on Titanium Dioxide (110) Surface. *J. Chem. Phys.* **2009**, *130*, 124502.

[12] Henderson, M. A.; An HREELS and TPD Study of Water on TiO_2(110): The Extent of Molecular *versus* Dissociative Adsorption. *Surf. Sci.* **1996**, *355*, 151-166.

[13] Bohm, D.; Quantum Theory, Dover New York, **1989**.